ELSEVIER

PII: S0032-3861(96)00676-3

Polymer Vol. 38 No. 7, pp. 1573–1580, 1997

0032-3861/97/$17.00 + 0.00

Gas transport properties of poly(phenylene thioether imide)s

Z.-K. Xu*, M. Böhning, J. D. Schultze, G.-T. Li and J. Springer†
Technische Universität Berlin, Institut für Technische Chemie, Straße des 17. Juni 135, 10623 Berlin, Germany

and F. P. Glatz and R. Mülhaupt
Freiburger Materialforschungszentrum and Institut für Makromolekulare Chemie, Stefan-Meier-Straße 31, 79106 Freiburg i.Br., Germany
(Received 18 August 1995; revised 6 February 1996)

Gas transport of carbon dioxide, oxygen, nitrogen and methane gases in a series of poly(phenylene thioether imide)s based on 2,2-bis(3,4-decarboxyphenyl) hexafluoropropane dianhydride and diamine-terminated oligo(phenylene thioether)s has been investigated. The effects of the oligo(phenylene thioether) length on the gas permeabilities and diffusivities were determined and correlated with chain packing of the polymers. The incorporation of a long oligo(phenylene thioether) segment in the polymer backbone decreases gas permeability and permselectivity simultaneously. The decreases in permeability coefficients can be related to decreases in both the diffusion coefficients and the solubility coefficients of all the gases. Finally, the physical and gas transport properties are simply compared between poly(phenylene thioether imide)s and poly(phenylene thioether).

(Keywords: membrane gas separation; gas permeation; polyimide)

INTRODUCTION

The control of gas permeability and permselectivity of polymer membranes has become a subject of intense research with worldwide participation in both industrial and academic laboratories because of its importance for the development of new membrane separation processes and for the improvement of economics[1–5]. To achieve such control, it is necessary for us to have a good understanding of the relationships between the properties of the polymers and their gas permeability. Thus, hundreds of publications and patents on the synthesis, structure and gas transport properties of polymer materials have appeared over the past decade. Special attention[6–30] has been focused on the development of high glass transition temperature amorphous polymers, such as polyaramides[6,7], polysulfones[8–10], polycarbonates[10–13] and polyimides[14–29], which have led to a new generation of gas-separation membrane materials. Among these high-performance polymers, it was reported recently that polyimides with 2,2-bis(3,4-decarboxyphenyl) hexafluoropropane dianhydride (6FDA) exhibit both a high gas-permeability and a high gas-permselectivity[21–29].

The most desirable gas separation membrane materials should have high permeability and high permselectivity, and also high mechanical and thermal stability. However, structural modifications which lead to increases in polymer permeability usually result in losses in permselectivity and vice versa. This so-called 'trade-off' relationship is well described in the literature[3,5]. Expanding the performance envelope generally defined by this 'trade-off' relationship is one goal of current research efforts.

A fundamental objective of our research has been to combine the typical properties of 6FDA-based polyimides with the properties of other glassy polymers, such as polysulfone[29] and polytetrafluoroethylene (PTFE)[30]. In the present work, permeability coefficients and diffusion coefficients of CO_2, O_2, N_2, and CH_4 through amorphous films of four 6FDA-based poly(phenylene thioether imide)s differing in their phenylene thioether length were measured to investigate the effect of molecular structure on permeability and permselectivity.

EXPERIMENTAL

Material

The dianhydride monomer used in this study was 2,2-bis(3,4-decarboxyphenyl) hexafluoropropane dianhydride (6FDA). This monomer was supplied by Hoechst AG and used without further purification. The diamine monomers were the diamine-terminated oligo(phenylene thioether)s which were readily synthesized by means of aromatic nucleophilic displacement reactions of dibromo-terminated oligo(phenylene thioether)s and 4-aminothiophenol. The poly(phenylene thioether imide)s (PPTI) with one, two, three and four units of phenylene thioether were synthesized by condensation polymerization from the above monomers followed by a cyclodehydration reaction, as reported in a previous communication[31]. The chemical structure and designation of the polymers studied here are shown in *Figure 1*.

* Permanent address: Department of Polymer Science & Engineering, Zhejiang University, 310027 Hangzhou, P.R. China
† To whom correspondence should be addressed

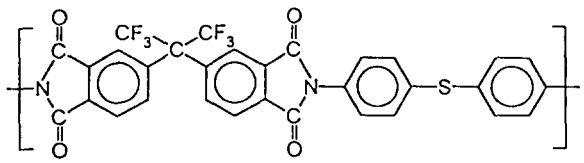

6FDA/PPTI-1

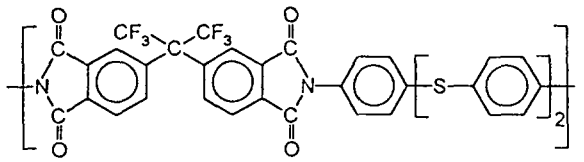

6FDA/PPTI-2

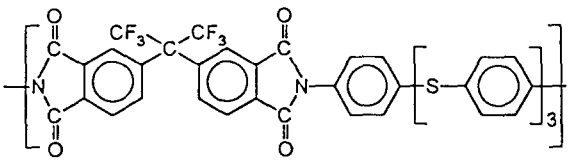

6FDA/PPTI-3

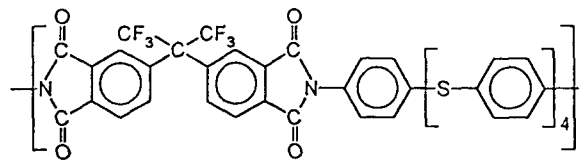

6FDA/PPTI-4

Figure 1 Molecular structure and designation of the 6FDA-poly(phenylene thioether imide)s studied

Carbon dioxide, oxygen, nitrogen and methane were purchased from Messer Griesheim GmbH. These gases were stated by the supplier to be at least 99.5% pure and were used without further purification.

Film preparation

The 6FDA-poly(phenylene thioether imide)s (6FDA-PPTI) were used in the form of nonporous planar membranes which were cast from 20 wt% DMF solutions at room temperature on glass plates and dried for 24 h at 100°C under vacuum. The films thus obtained were removed from the glass plates and dried for another 24 h at 100°C under vacuum. No trace of solvent could be detected from differential scanning calorimetry (d.s.c.) scans. The thickness of the dry films used for the permeability and diffusity measurements varied from 20 to 40 μm with individual uniformities better than ±6%. Poly(1,4-phenylene thioether) (PPT) (or poly(1,4-phenylene sulfide)) films with 100 μm (±4%) thickness were obtained from Bayer AG. No indications of crystallinity were observed in d.s.c. scans or wide-angle X-ray diffraction spectra for the 6DFA/PPTI films, while the PPT films exhibit a degree of crystallinity of about 5% according to density measurements[32–34].

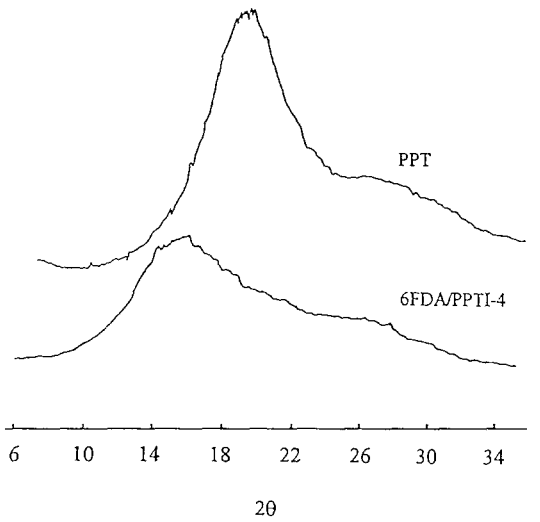

Figure 2 WAXD scan of 6FDA-PPTI-4 and poly(1,4-phenylene thioether) (PPT)

Thermal and physical characterization

Glass transition temperatures were determined using Rheometrix solid analyzer (RSA II) at a heating rate of 10°C min^{-1} and an oscillation frequency of 1 Hz[29]. Wide-angle X-ray diffraction (WAXD) measurements were taken for each polymer at a CuKα wavelength λ of 1.54 Å on a Philips X-ray diffractometer. The corresponding d-spacing values which provide a measure of intersegmental distance between polymer backbones were calculated from the diffraction peak maxima through the Bragg equation, $d = \lambda/2\sin\theta$[35,36], where λ is the wavelength of the radiation and 2θ is the angle of maximum intensity in the amorphous halo exhibited by these polymers. Polymer density was determined by flotation of small film samples in a density gradient column, which was maintained at 23 ± 0.1°C. Aqueous calcium nitrate solution was used to provide the density gradient.

The packing density (PD), which is a related measure of chain packing, was calculated using[37]:

$$\mathrm{PD} = V/(V - V_{\mathrm{w}}) \qquad (1)$$

where V is the polymer specific volume, and V_{w} is the specific van der Waals volume calculated by the group contribution method of van Krevelen[38]. The cohesive energy (E_{coh}), which could be considered as a measure of interaction of polymer chains and mainly determined by the ability of the polymer chains to perform segmental motions, were also calculated from the group contribution method of van Krevelen. The tabulation of Fedors[38] was used to calculate E_{coh}.

Pure gas permeability determination

Pure gas permeability coefficients for CO_2, O_2, N_2 and CH_4 gases were measured at 35°C between 1–10 atm and at 10 atm for different temperatures between 35–75°C using the standard techniques employed in our laboratory, based on the time-lag method[29–30,39]. Effective gas diffusion coefficients were estimated from time-lag data at upstream pressures of 10 atm and a temperature of 35°C by the relation $D = l^2/6\theta$, where l is the film thickness and θ is the time-lag[39]. The apparent solubility coefficients of the four gases in each polymer

Table 1 Physical and chemical properties of the polymers studied

Polymer	T_g (°C)	Density ($g\,cm^{-3}$)	d-spacing (C)	PD	FFV	E_{coh}^{-1} ($kJ\,mol^{-1}$)
6FDA/PPTI-1	292	1.4373	5.51	2.820	0.1614	253.88
6FDA/PPTI-2	257	1.4179	5.50	2.834	0.1587	299.97
6FDA/PPTI-3	233	1.3980	5.46	2.824	0.1603	346.06
6FDA/PPTI-4	216	1.3956	4.94	2.865	0.1583	392.15

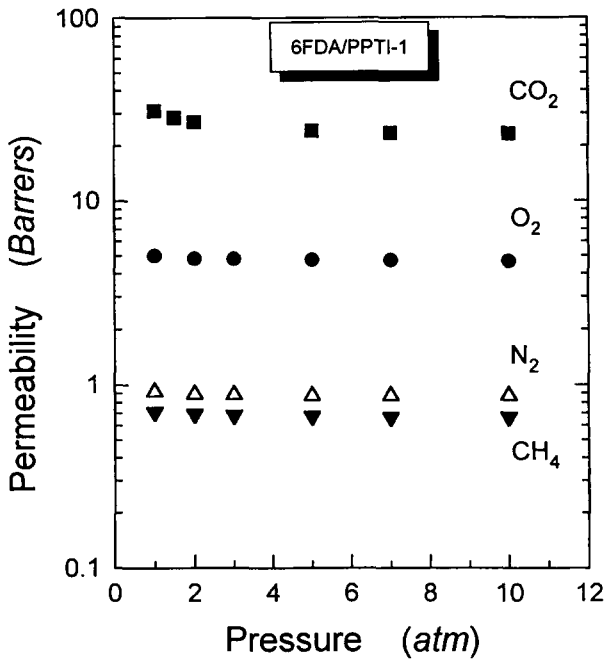

Figure 3 Dependence of gas permeabilities on upstream pressure for 6FDA/PPTI-1 at 35°C

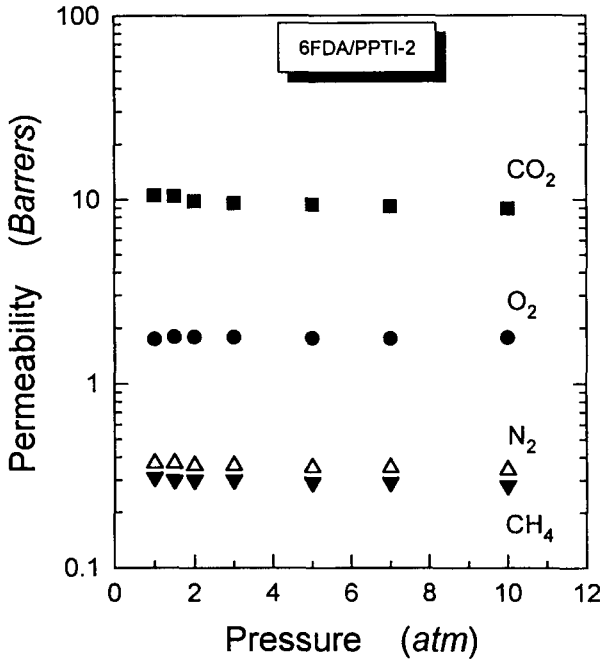

Figure 4 Dependence of gas permeabilities on upstream pressure for 6FDA/PPTI-2 at 35°C

film were calculated from the relationship $S = P/D$, where S is the solubility coefficient and P the permeability coefficient determined from the steady state of the time-lag experiment[34,39]. Ideal permselectivities ($\alpha_{A/B}$) were calculated from:

$$\alpha_{A/B} = P_A/P_B \quad (2)$$

where P_A and P_B are the permeabilities of pure gas A and B, respectively. Assuming the absence of both penetrant/penetrant and penetrant/polymer interactions, this ideal permselectivity should provide a useful estimation of the separation performance for the actual gas mixture.

RESULTS AND DISCUSSION

Characterization of poly(phenylene thioether imide)s

The physical properties of the 6FDA-based poly(phenylene thioether imide) films are shown in *Table 1*. It can be seen that an increase in the length of the oligo(phenylene thioether) segment in the diamine moieties led to a reduction of the glass transition temperature (T_g) and the density of the polymers. There is no long-range order for these amorphous materials, therefore, broad and structureless peak characteristics of the WAXD spectra were observed for each polymer. The diffraction pattern of 6FDA/PPTI-4 is given in *Figure 2* as a typical set. For the reason of comparison conducted below, the diffraction pattern of PPT is included in this figure, also revealing no sharp single reflexes, indicating an almost amorphous material with very low and poorly ordered overall crystallinity. The other poly(phenylene thioether imide)s exhibited diffraction patterns very similar in shape to that for 6FDA/PPTI-4 in *Figure 2*. The most prominent WAXD peak in the spectra of amorphous glassy polymers is often used to estimate the average interchain spacing distances (d-spacing). These values were also calculated using the Bragg equation and are listed in *Table 1*.

With the number of units in the oligo(phenylene thioether) structure increased from one to four, the d-spacing decreases from 5.51Å to 4.94Å. The calculated packing density (PD) and molar cohesive energy (E_{coh}) increase from 2.820 to 2.865 and from 253 $kJ\,mol^{-1}$ to 392 $kJ\,mol^{-1}$, respectively, while the glass transition temperature (T_g) is lowered from 292°C to 216°C. All these results indicate that an increase in the length of the oligo(phenylene thioether) structure in the polymer backbone results in an increase in both segmental mobility and chain packing.

Pure gas transport properties

The effect of upstream driving pressure on the permeability coefficients for these materials are given in *Figures 3–6*. As for most polyimides reported in the

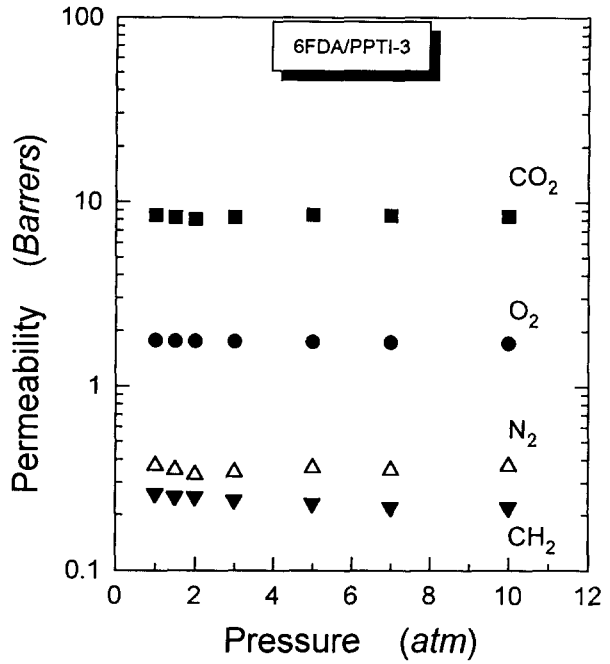

Figure 5 Dependence of gas permeabilities on upstream pressure for 6FDA/PPTI-3 at 35°C

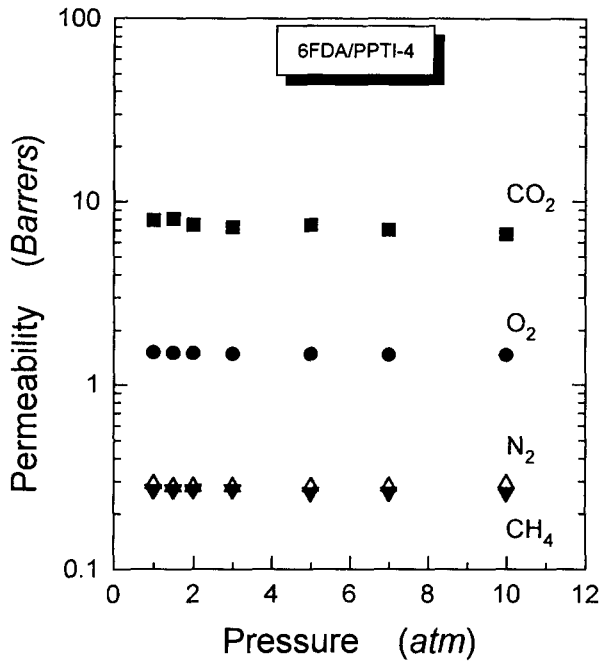

Figure 6 Dependence of gas permeabilities on upstream pressure for 6FDA/PPTI-4 at 35°C

Table 2 Permeabilities[a] and permselectivities of 6FDA/PPTI membranes at 35°C and 10 atm

Polymer	P_{O_2}	P_{N_2}	P_{O_2}/P_{N_2}	P_{CO_2}	P_{CH_4}	P_{CO_2}/P_{CH_4}
6FDA/PPTI-1	4.66	0.87	5.36	23.11	0.66	34.79
6FDA/PPTI-2	1.77	0.34	5.21	8.92	0.28	31.43
6FDA/PPTI-3	1.72	0.37	4.65	8.37	0.22	34.64
6FDA/PPTI-4	1.46	0.29	5.07	6.62	0.26	25.42

[a] Barrers (10^{-10} × cm^3(STP) cm^{-2} s^1 cm^{-1} Hg^{-1})

Table 3 Diffusivities[a] and diffusion selectivities of 6FDA/PPTIs at 35°C and 10 atm

Polymer	D_{O_2}	D_{N_2}	D_{O_2}/D_{N_2}	D_{CO_2}	D_{CH_4}	D_{CO_2}/D_{CH_4}
6FDA/PPTI-1	6.80	1.36	4.99	3.54	0.39	9.07
6FDA/PPTI-2	3.71	1.04	3.57	1.71	0.22	7.62
6FDA/PPTI-3	3.71	–	–	1.53	0.19	8.11
6FDA/PPTI-4	4.13	0.82	5.06	1.69	0.28	6.09

[a] 10^{-8} cm^2 s^{-1}

Table 4 Solubilities[a] and solubility selectivities of 6FDA/PPTIs at 35°C and 10 atm

Polymer	S_{O_2}	S_{N_2}	S_{O_2}/S_{N_2}	S_{CO_2}	S_{CH_4}	S_{CO_2}/S_{CH_4}
6FDA/PPTI-1	0.52	0.49	1.07	4.96	1.29	3.84
6FDA/PPTI-2	0.36	0.26	1.36	3.96	0.96	4.12
6FDA/PPTI-3	0.35	–	–	4.15	0.89	4.64
6FDA/PPTI-4	0.27	0.27	1.00	2.98	0.71	4.18

[a] cm^3(STP) cm^{-3} (polymer) atm^{-1}

literature[16,28], the permeability coefficients are essentially independent of upstream pressure or tend to decrease slightly with increasing pressure. The permeability coefficients and ideal separation factors for the four gases at 35°C and 10 atm upstream pressure are shown in *Table 2*, while diffusivity coefficients, diffusivity selectivities, solubility coefficients and solubility selectivities are presented in *Table 3* and *Table 4*, respectively. It is well known that glassy polymers are not in a state of equilibrium and the prior history (thermal, mechanical, processing, and even gas exposure) influences current and future performance[1,2]. Manifestations of this also

include time-dependent and hysteretic behaviour. For this reason, there is little difference between the permeability data obtained in this study and those of our previous study[29].

Figures 3–6 and *Table 2* show that the permeability coefficients for this series of polyimides decrease in the order of gases: $P(CO_2) > P(O_2) > P(N_2) > P(CH_4)$. This is also the order of increasing 'kinetic' diameters calculated from the minimum cross-sectional diameters of the penetrant molecules[40]. However, for all four poly(phenylene thioether imide)s studied in this work, the diffusion coefficients rank in the following order: $D(O_2) > D(CO_2) > D(N_2) > D(CH_4)$. The relative magnitudes of D for CO_2 and O_2 are anomalous from their 'kinetic' diameter, σ_K, because $D(O_2) > D(CO_2)$ whereas $\sigma_K(O_2) > \sigma_K(CO_2)$[40]. Similar behaviour has been observed for other types of glassy polymers including poly(imide)s[18,21,23,24,28], poly(carbonate)s[10–13], poly(sulfone)s[8–10] and poly(arylate)s[41]. Under normal conditions, the very high solubility of CO_2 in these polymer materials causes the CO_2 permeability to be higher than that of O_2 because the permeability coefficient of a gas is the product of diffusivity coefficient (D) and solubility coefficient (S).

Table 2 also shows that the 6FDA/PPTI-1 polyimide has both the highest permeabilities and the highest permselectivities for the oxygen/nitrogen and carbon dioxide/methane gas pairs respectively among this homologous series of polyimides. These results are expected since the 6FDA/PPTI-1 is both more open and more rigid than its homologues, as indicated by the lower packing density (PD) and the higher T_g values. With the exception of 6FDA/PPTI-3, an increase in the segment length of the flexible oligo(phenylene thioether) led to simultaneous decreases in gas permeabilities and permselectivities. For example, the permeability coefficients of CO_2 and O_2 in 6FDA/PPTI-1 are about 2.6 times larger than those in 6FDA/PPTI-2, while the permselectivities of oxygen/nitrogen and carbon dioxide/methane systems in the former are 2.9% and 9.8% higher than those of the latter. As explained in more detail later, the decreases in permeabilities is consistent with the calculated fractional free volume (*FFV*) values reported in *Table 1*, the free volume of 6FDA/PPTI-1 is greater than that of 6FDA/PPTI-2, and gas permeability coefficients are universally understood to be quite sensitive to the free volume of glassy amorphous polymers. The decreases in permselectivities, however, are not consistent with the commonly observed 'trade-off' between permeability and permselectivity, that is, polymers that are more permeable tend to exhibit lower permselectivities and vice versa[5]. A general hypothesis which was proposed in recent years[41] is that an optimal distribution of polymer free volume is needed to achieve both a high permeability and a high permselectivity. The alternation of packing disruptive and easily packable segments in the polymer backbone has been suggested as one possible route to obtain such favourable distribution. However, it was found that packing effects or rigid polymer chains mainly influence the permeability while the rotation around flexible linkages in the polymer backbone affects the permselectivity[41], i.e. permselectivity increases with reduction of rotational mobility. For the 6FDA-based poly(phenylene thioether imide)s studied here, the rigid 6FDA group is the packing disruptive part whereas the flexible oligo(phenylene thioether) segment is the more packable part in the polymer backbone. Introducing phenylene thioether units into the polyimide's structural unit results, due to higher flexibility of the polymer backbone, in an altered chain packing and thus a different free volume distribution. However, the rotational mobility is changed at the same time.

If this is the situation, it seems that one unit ($n = 1$) of the oligo(phenylene thioether) in the polymer backbone is appropriate to obtain a favourable free volume distribution in this kind of poly(imide)s.

As can be seen from the values listed in *Table 3* and *Table 4*, the decreases in gas permeabilities with the increases in the segment length of oligo(phenylene thioether) is a result of a decrease in both diffusion coefficients and solubility coefficients. For example, there are 52% and 45% decreases in the diffusion coefficients of CO_2 and O_2 from 6FDA/PPTI-1 to 6FDA/PPTI-2 with corresponding 20% and 31% decreases in solubility coefficients, respectively. For the carbon dioxide/methane gas pair, however, the changes in permselectivity are dominated mainly by variations in the diffusivity selectivity. The variations in the solubility selectivities are relatively small in this series of polymers because the S atoms and the phenyl ring groups do not give rise to strong physical interactions with any of the gases studied.

Free volume analysis

In order to understand the gas permeation mechanism, free volume theory is often applied to glassy amorphous polymers[9–13,18,21,23,41]. According to this theory which was developed by Fujita[42], gas diffusivity D is assumed to depend on free volume:

$$D = A\exp(-B/FFV) \tag{3}$$

where A and B are characteristic constants which are independent of the penetrant concentration and temperature, *FFV* is the fractional free volume of the polymer. This relation typically provides a good description of gas diffusivity in a family of polymers[18,21,43,44]. Lee[43] suggested that solubility would not be a strong function of free volume and, therefore, the gas permeability P and *FFV* should be related by:

$$P = A'\exp(-B'/FFV) \tag{4}$$

where A' and B' are constants. Using this correlation, a number of investigators[9–13,41] have pointed out in recent years that the gas permeability of glassy polymers is reasonably well correlated with their *FFV*, at least within specific classes of materials. Thus, we also calculated the *FFV* and investigated the relationship between *FFV* and gas permeability.

The measured density for each polymer was used to estimate the *FFV* from:

$$FFV = (V - 1,3V_w)/V \tag{5}$$

where V is the polymer specific volume, and V_w is the specific van der Waals volume calculated using the group contribution method of van Krevelen[38]. The calculated polymer fractional free volumes are listed in *Table 1*. With the exception of 6FDA/PPTI-3, the *FFV* is decreased by the increase of the oligo(phenylene thioether) length. The permeability coefficients of CO_2,

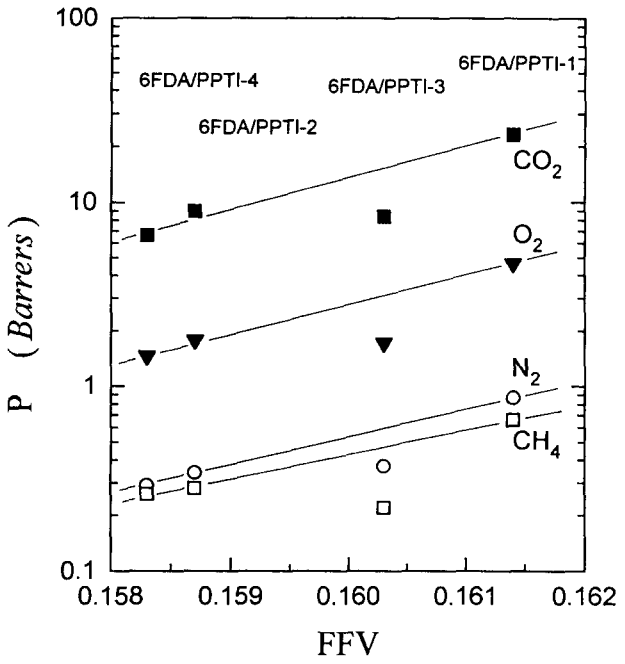

Figure 7 Dependence of gas permeabilities on fractional free volume (*FFV*)

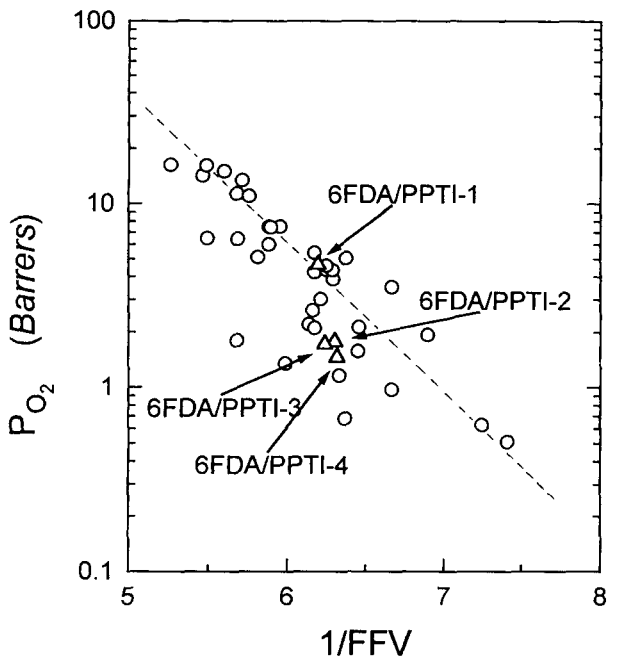

Figure 8 Relationship between the O_2 permeability and the fractional free volume of the 6FDA-based polyimides at 35°C (data from refs 21–29 and this study)

Table 5 Activation energies of permeation and pre-exponential factors for four penetrants in 6FDA/PPTIs

Polymer	CO_2	O_2	N_2	CH_4
E_p (kcal mol^{-1})				
6FDA/PPTI-1	1.90	3.67	4.74	5.65
6FDA/PPTI-2	2.69	4.52	5.63	6.52
6FDA/PPTI-4	3.49	4.95	7.09	–
P_0 (Barrers)				
6FDA/PPTI-1	5.15×10^2	1.87×10^3	2.01×10^3	6.74×10^3
6FDA/PPTI-2	7.23×10^2	2.85×10^3	3.36×10^3	1.18×10^4
6FDA/PPTI-4	1.98×10^3	4.75×10^3	6.08×10^3	–

O_2, N_2 and CH_4 are in good agreement with the fractional free volume, as shown in *Figure 7*. The reason for the anomalous results of 6FDA/PPTI-3 is unclear at present. To elucidate this, molecular structure characterizations, especially spectroscopy analyses, are needed. In this context also it has to be taken into account that a real structure may be represented by the calculated parameters *FFV* and *PD* to a different extent due to distortions of the polymer backbone and local packing effects.

In recent years, permeability coefficients for O_2 at 35°C have been reported for many 6FDA-based polyimides in the amorphous state[21–29]. A plot of the logarithm of these oxygen permeability coefficients versus the reciprocal of the fractional free volume (*FFV*) according to equation (4) is given in *Figure 8*. All values for *FFV* were calculated according equation (5) using the group contribution tabulation of van Krevelen[38]. Although the correlation of log P_{O_2} with $1/FFV$ holds roughly for this kind of polymers with widely differing values of *FFV*, there is a significant difference in permeability with similar values of $1/FFV$. For the 6FDA-based poly(phenylene thioether imide)s studied in the present work, it seems that the P_{O_2} value for 6FDA/PPTI-1 was as large as expected from the calculated value of *FFV*, whereas those for the other 6FDA-based poly(phenylene thioether imide)s were lower than expected. This may show that a linear relationship as proposed by equation (4) is valid only for a particularly limited group of structurally related polymers. Therefore, a free volume approach to modelling gas transport in polymer materials has merit, but also has room for improvement and so investigation continues.

Effect of temperature on gas permeabilities

Gas permeability coefficients generally follow an Arrhenius relationship[45]:

$$P = P_0 \exp(-E_p/RT) \quad (6)$$

where P_0 is a pre-exponential factor, E_p is the activation energy for permeation, R is the ideal gas constant, and T is the temperature. *Figure 9* shows the permeability coefficients for various gases in 6FDA-PPTI-1, 6FDA-PPTI-2 and 6FDA-PPTI-4 plotted in Arrhenius coordinates over the temperature range 35–75°C. Activation energies and pre-exponential factors calculated from these plots are shown in *Table 5*. In every case, the activation energies for permeation increase with the

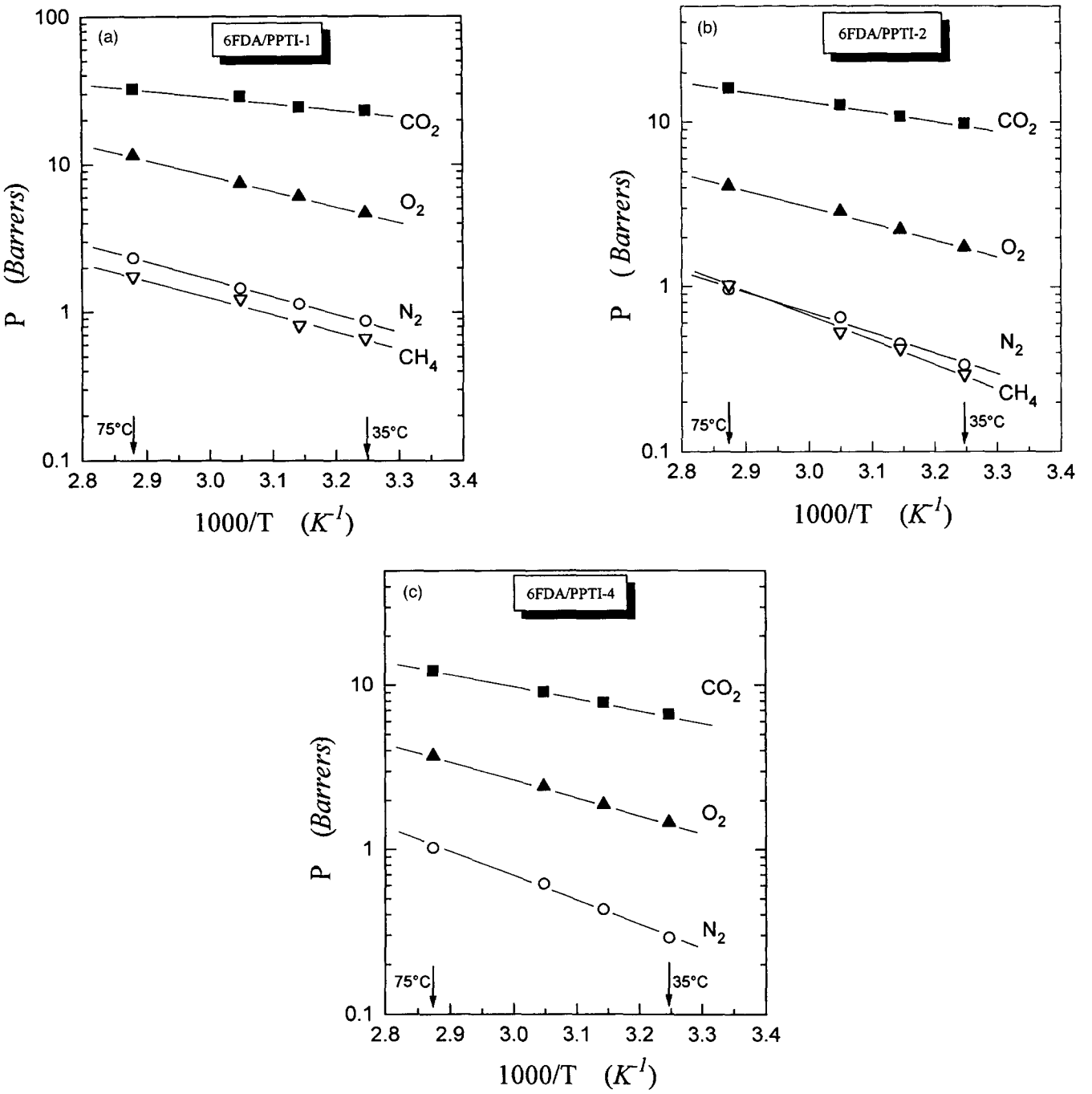

Figure 9 Dependence of gas permeabilities on temperature: (a) 6FDA/PPTI-1; (b) 6FDA/PPTI-2; (c) 6FDA/PPTI-4

Table 6 Comparison of 6FDA/PPTI-4 and PPT

Polymer	T_g (°C)	ρ (g cm^{-3})	d-spacing (C)	PD	FFV	P_{CO_2}	P_{CH_4}	P_{CO_2}/P_{CH_4}	$E_p(CO_2)$ (kcal mol^{-1})
6FDA/PPTI-4	216	1.3956	4.94	2.86	0.1583	6.62	0.26	25.42	3.49
PPT	90	1.3160	4.30	2.93	0.1442	0.14	0.0075	18.67	6.43

increase of the oligo(phenylene thioether) length. This result is expected because it is known that a glassy polymer with a higher T_g tends to have a lower E_p within a family of polymers. Moreover, the E_p and P_0 values provide a convenient method to calculate permeabilities for each polymer–penetrant pair at a given temperature. However, these parameters are applicable only within the respective temperature range in which no significant thermal transition takes place for each polymer.

Comparison of 6FDA/PPTI-4 polyimide and poly(1,4-phenylene thioether)

The potential possibilities using poly(1,4-phenyl thioether) (PPT) as gas separation membrane materials were explored by several investigators[34,36]. It is useful to compare the properties of the 6FDA/PPTI polyimides with those of PPT. 6FDA/PPTI-4 was selected as a representative to do such comparison owing to the longest oligo(phenylene thioether) segment in its polymer backbone. As can be seen from *Figure 2*, the WAXD scan for amorphous PPT shows a peak with a maximum at 4.30Å *d*-spacing, while the scan for 6FDA/PPTI-4 shows a very broad peak with a maximum at 4.94Å *d*-spacing. In addition to the different *d*-spacing values, the broader X-ray peak for 6FDA/PPTI-4 also suggests that the polymer chain packing and thus the distribution of free volume may be somewhat different for 6FDA/PPTI-4 than for PPT. The PPT film was found to have a density of 1316 g cm^{-3}, which is within the same range as reported in the literature[32,34,46] for the almost amorphous material and is 6% less than that of 6FDA/PPTI-4, as presented in *Table 6*. The greater rotational mobility about the thioether linkage of PPT allow the polymer chains to pack more densely and result in a higher *PD* and lower *FFV* than 6FDA/PPTI-4. Conversely, the introduction of bulky, sterically hindered groups such as 6FDA within the polymer backbone tends to increase the inhibitions to segmental mobility which are reflected in an increased T_g. Therefore, the T_g and *FFV* values for 6FDA/PPTI-4 are about 130°C and 10% higher, respectively, than those for PPT.

As expected from the molecular structure and physical properties, 6FDA/PPTI-4 polyimide shows both higher permeabilities and permselectivity toward carbon dioxide/methane system than PPT. Moreover, the activation energy permeation of CO_2 for the former is 84% lower than that of the latter.

ACKNOWLEDGEMENT

One of the authors, Zhi-Kang Xu, is thankful to Zentrum für Technologische Zusammenarbeit of Technische Universität Berlin for a fellowship.

REFERENCES

1 Kesting, R. E. and Fritzsche, A. K. 'Polymeric Gas Separation Membranes', John Wiley & Sons, Inc. New York, 1993
2 Paul, D. R. and Yampol'skii, Yu. P. (Eds) 'Polymeric Gas Separation Membranes', CRC Press, Inc. Boca Raton, 1994
3 Stern, S. A. *J. Membr. Sci.* 1994, **94**, 1
4 Koros, W. J. and Fleming, G. K. *J. Membr. Sci.* 1993, **83**, 1
5 Robeson, L. M. *J. Membr. Sci.* 1991, **62**, 165
6 Hoehn, H. H. *ACS Symp. Ser.* 1985, **269**, 81
7 Ghosal, K. Freeman, B. D. Chern, R. T. Alverez, J. C. de la Campa, J. G. Lozano, A. E. and de Abajo, J. *Polymer* 1995, **36**, 793
8 McHattie, J. S. Koros, W. J. and Paul, D. R. *Polymer* 1991, **32**, 840
9 Aitken, C. L. Koros, W. J. and Paul, D. R. *Macromolecules* 1992, **25**, 3425
10 Aguilar-Vega, M. and Paul, D. R. *J. Polym. Sci., Polym. Phys. Edn.* 1993, **31**, 1599
11 Schimdhauser, J. C. and Longley, K. L. *J. Appl. Polym. Sci.* 1991, **39**, 2083
12 Costello, L. M. and Koros, W. J. *J. Polym. Sci., Polym. Phys. Edn.* 1994, **32**, 701
13 Hellums, M. W. Koros, W. J. Husk, G. R. and Paul, D. R. *J. Appl. Polym. Sci.* 1991, **43**, 1977
14 Sykes, G. F. and St. Clair, A. K. *J. Appl. Polym. Sci.* 1986, **32**, 3725
15 Kim, T. H. Koros, W. J. Husk, G. R. and O'Brien, K. C. *J. Membr. Sci.* 1988, **37**, 45
16 Stern, S. A. Mi, Y. Yamamoto, H. and St. Clair, A. K. *J. Polym. Sci., Polym. Phys. Edn.* 1989, **27**, 1887
17 Mi, Y. Stern, S. A. and Trohalaki, S. *J. Membr. Sci.* 1993, **77**, 41
18 Tanaka, K. Okano, M. Toshino, H. Kita, H. and Okamoto, K. *J. Polym. Sci., Polym. Phys. Edn.* 1992, **30**, 907
19 Matsumoto, K. Xu, P. and Nishikimi, T. *J. Membr. Sci.* 1993, **81**, 15
20 Langsam, M. and Burgoyne, W. F. *J. Polym. Sci., Polym. Chem. Edn.* 1993, **31**, 909
21 Tanaka, K. Kita, H. Okano, M. and Okamoto, K. *Polymer* 1992, **33**, 585
22 Costello, L. M. and Koros, W. J. *J. Polym. Sci., Polym. Phys. Edn.* 1995, **33**, 135
23 Coleman, M. R. and Koros, W. J. *J. Polym. Sci., Polym. Phys. Edn.* 1994, **32**, 1915
24 Coleman, M. R. and Koros, W. J. *J. Membr. Sci.* 1990, **50**, 285
25 Matsumoto, K. and Xu, P. *J. Appl. Polym. Sci.* 1993, **47**, 1961
26 Coleman, M. R. Kohn, R. and Koros, W. J. *J. Appl. Polym. Sci.* 1993, **50**, 1059
27 Zoia, G. Stern, S. A. St. Clair, A. K. and Pratt, J. R. *J. Polym. Sci., Polym. Phys. Edn.* 1994, **32**, 53
28 Stern, S. A. Liu, Y. and Feld, W. A. *J. Polym. Sci., Polym. Phys. Edn.* 1993, **31**, 939
29 Glatz, F. P. Mülhaupt, R. Schultze, J. D. and Springer, J. *J. Membr. Sci.* 1994, **90**, 151
30 Steinhauser, N. Mülhaupt, R. Hohmann, M. and Springer, J. *Polym. Adv. Technol.* 1994, **5**, 438
31 Mülhaupt, R. Glatz, F. P. Schultze, J. D. and Springer, J. *Polym. Prepr. Am. Chem. Soc. Div. Polym.* 1992, **33**, 203
32 Ito, M. Porter, R. S. *J. Polym. Sci., Polym. Phys. Edn.* 1985, **23**, 245
33 Maemura, E. Cakmak, M. White, J. L. *Int. Polym. Process* 1988, **3**, 79
34 Schultze, J. D. Ph.D. dissertation D83. Technische Universitaet Berlin, 1992
35 Boehme, R. F. and Cargill III, G. S. in 'Polyimides' (Ed. K. L. Mittal), Plenum Press, New York, NY, 1984
36 Schwarts, L. H. and Cohen, J. B. 'Diffraction from Materials', Academic Press, New York, NY, 1977, Ch. 3
37 Chern, R. T. Sheu, F. R. Jia, L. Stannett, V. T. and Hopfenberg, H. B. *J. Membr. Sci.* 1987, **35**, 103
38 van Krevelen, D. W. 'Properties of Polymers', 3rd Edn. Elsevier, New York, 1992
39 Crank, J. 'The Mathematics of Diffusion', 2nd Edn. Oxford Univ. Press, 1975
40 Breck, D. W. 'Zeolite Molecular Sieves', John Wiley & Sons, New York, 1974, Ch. 8
41 Pixton, M. R. and Paul, D. R. *J. Polym. Sci., Polym. Phys. Edn.* 1995, **33**, 1135
42 Fujita, H. in 'Diffusion in Polymers' (Eds J. Crank and G. S. Park), Academic Press, New York, 1968, p. 75
43 Lee, W. M. *Polym. Eng. Sci.* 1980, **20**, 65
44 McHattie, J. S. Koros, W. J. and Paul, D. R. *Polymer* 1992, **33**, 1701
45 Stannett, V. T. 'Diffusion in Polymers', John Wiley & Sons, New York, 1971
46 Aguiler-Vega, M. and Paul, D. R. *J. Polym. Sci., Polym. Phys. Edn.* 1993, **31**, 1577